

Effect of polydispersity on the phase behavior of non-additive hard spheres in solution, part II

Luka Sturtewagen and Erik van der Linden

*Laboratory of Physics and Physical Chemistry of Foods,
Wageningen University, Bornse Weiland 9, 6708 WG Wageningen, The Netherlands*

We study the theoretical phase behavior of an asymmetric binary mixture of hard spheres, of which the smaller component is monodisperse and the larger component is polydisperse. The interactions are modeled in terms of the second virial coefficient and can be additive hard sphere (HS) or non-additive hard sphere (NAHS) interactions. The polydisperse component is subdivided into two sub-components and has an average size ten or three times the size of the monodisperse component. We give the set of equations that defines the phase diagram for mixtures with more than two components in a solvent. We calculate the theoretical liquid-liquid phase separation boundary for two phase separation (the binodal) and three phase separation, the plait point, and the spinodal. We vary the distribution of the polydisperse component in skewness and polydispersity, next to that we vary the non-additivity between the sub-components as well as between the main components. We compare the phase behavior of the polydisperse mixtures with binary monodisperse mixtures for the same average size and binary monodisperse mixtures for the same effective interaction. We find that when the compatibility between the polydisperse sub-components decreases, three-phase separation becomes possible. The shape and position of the phase boundary is dependent on the non-additivity between the sub-components as well as their size distribution. We conclude that it is the phase enriched in the polydisperse component that demixes into an additional phase when the incompatibility between the sub-components increases.

Keywords: Polydispersity, hard spheres, phase behavior, virial coefficient, non-additive hard sphere interaction

I. INTRODUCTION

In the study of the phase behavior of binary mixtures, the components are usually assumed to be pure and monodisperse, however in nature most components are not that neatly monodisperse. Many components show size and charge variation or contain hard to remove particles that can influence their phase behavior in binary mixtures. In their experimental work, Sager [1] reported that even small impurities can lead to drastic shifts in the position of the phase boundary. Next to that the compatibility between components can be depended on the temperature [2], salt concentration or pH of the solution[3].

Two different physical mechanisms drive the phase separation between hard spheres. The first one involves only excluded volume interactions. In this mechanism the minimal distance between the particles is determined by the sum of their respective radii [4]. This is the typical additive hard sphere interaction (HS). With this mechanism, phase separation is driven by a size asymmetry between the particle sizes [5]. This asymmetry leads to depletion of small spheres around the large spheres and as a result to an effective attraction (depletion interaction) between the larger spheres [6]. The other mechanism is when the distance between the particles of a different species can be larger or smaller than the sum of their respective radii. This is referred to as non-additive hard sphere (NAHS) interaction. Previous research has shown that already at small degrees of non-additivity it becomes possible for components with no size asymmetry to demix [7] [8]. Either way, upon phase separation, the mixture will demix into two (or more) phases, each enriched in

one of the components. In the previous article, we focused on the first type of interaction [9]. We investigated the influence of size polydispersity on the phase behavior of an additive binary asymmetric mixture. In this work we will focus on the second type, binary (polydisperse) mixtures where the distance between the particles of different species can be larger or smaller than the sum of their respective radii.

Piech and Walz [10] studied the effect of size polydispersity and charge heterogeneity on the depletion interaction in a colloidal system. They found that the size distribution in the larger particle had a different effect on the depletion attraction for charged and non-charged hard sphere systems. For the depletion attraction decreased between the larger particles at constant volume fraction due to the polydispersity. This effect was further enhanced by the presence of charge. Polydispersity significantly lowers the magnitude of the repulsive barrier.

The non-additivity is usually described by the non-additivity parameter Δ (with $\Delta \geq -1$). When $\Delta = 0$ the mixture has additive hard sphere interaction and the closest approach of the particles is the sum of their radii. When $\Delta < 0$ the two particles experience more attraction and can come closer to each other than the sum of their radii, while when $\Delta > 0$ the two particles have more repulsion and their distance of closest approach is larger than the sum of their respective radii. It is clear that this can have enormous effects on their phase behavior. Particles with a negative Δ tend to be more compatible with each other, while particles with a positive Δ are less compatible and tend to demix at lower concentrations. Already at the relatively low $\Delta = 0.1$, it becomes

possible for components with the same size to demix [11].

Paricaud [12] studied the phase behavior of polydisperse colloidal dispersions. Their mixture consisted of a monodisperse component and a polydisperse component. The interaction between the monodisperse and polydisperse components was assumed to be NAHS (with the same Δ for all polydisperse sphere), while the interaction between the polydisperse components amongst themselves was assumed to be additive HS. They find that the critical point of a polydisperse mixture is at lower solution pressure than for completely monodisperse mixtures. For mixtures with large variation in the size of the polydisperse mixtures they observe the possibility of a three phase system. The phase behavior of a colloid and a polydisperse polymer was studied by [13]. They used the Asakura-Osawa model for the interactions between the different components. They found that increasing the polydispersity increased also the extent of the fluid-fluid coexistence. They reason that the introduction of larger polymer coils is the driving force towards phase separation.

In this study we aim to get a better understanding of how non-additive interaction influences the phase behavior of binary mixtures with some polydispersity or impurities. We will study the position of the phase separation boundary, the spinodal, and the critical point. Next to that we aim to predict the fractionation of the polydisperse component between the different phases. We model the interactions between the different components using the second virial coefficient (II A). In section II B we describe the equations for the spinodal, in section II C we describe the equations for the critical point and finally in section II D we describe the equations defining the phase boundary. With the expressions in section II we have enough to calculate the phase diagram for a variety of mixtures described in section III. First we introduce non-additivity between the main components in the binary mixtures (III A), subsequently we introduce non-additivity between the sub-components in the polydisperse component (III B), and finally we combine both in section III C. In section III D we look into the fractionation of some of the mixtures from III B at a specific parent concentration.

II. THEORY

We show the equations used for the calculations of the phase diagram of the different studied systems: the set of equations defining the stability boundary, the critical point, and phase boundaries of a mixture. All sets of equations are solved in Matlab R2017b. For a more detailed derivation of the equations, we refer to [9].

A. Osmotic virial coefficient

The osmotic pressure, Π , of a solution at a temperature T , can be written as a virial expansion, similar to the virial expansion of the universal gas law for real gases [14]:

$$\beta\Pi = \rho + B_2(T, \mu_s)\rho^2 + B_3(T, \mu_s)\rho^3 + \dots \quad (1)$$

with $\beta = \frac{1}{kT}$, k the Boltzmann's constant, ρ the number density of the component $\left(\frac{N_\nu}{V}\right)$, B_2 the second virial coefficient, and B_3 the third virial coefficient. The second virial coefficient accounts for the increase in osmotic pressure due to particle pairwise interaction. The third virial coefficient accounts for the interaction between three particles in a variety of configurations. The equation can be expanded for higher densities with B_n , the n^{th} virial coefficient, which accounts for the interaction between n different particles.

In this work we will limit the virial expansion to the second virial coefficient, which is given by [15]:

$$B(T, \mu_s) = 2\pi \int_0^\infty r^2 (1 - \exp[-\beta W(r)]) dr \quad (2)$$

in which μ_s is the chemical potential of the solution, $W(r)$ is the interaction potential between the particles, and r is the distance.

For additive hard sphere (HS) interaction, the interaction potential for two particles (of the same species or different species) is given by:

$$W(r)_{HS} = \begin{cases} 0, & r > \sigma_{ij} \\ \infty, & r \leq \sigma_{ij} \end{cases} \quad (3)$$

with $\sigma_{ij} = (\sigma_i + \sigma_j)/2$, the distance between the centers of the two particles.

For non-additive hard spheres (NAHS), the distance of the closest approach of the centers of the two particles of different species can be closer or further than the distance between their centers [7]. The closest distance then becomes: $\sigma_{ij} = ((\sigma_i + \sigma_j)/2)(1 + \Delta)$, in which Δ (≥ -1) accounts for the non-additivity of the interaction between the particles. When $\Delta > 0$ the distance of closest approach of both spheres increases and when $\Delta < 0$ the distance of closest approach decreases compared to that due to HS interaction only. For additive hard sphere interaction $\Delta = 0$.

In a mixture with n distinguishable components in a solution, there are two main types of two particle interactions that can occur: between particles of the same species and particles of different species.

For the second virial coefficient given by eq. 2, using the interaction potential defined in eq. 3, we find:

$$B_{xx} = \frac{2\pi}{3}(\sigma_x)^3 \quad (4)$$

$$B_{xy} = \frac{2\pi}{3} \left(\left(\frac{\sigma_x + \sigma_y}{2} \right) (1 + \Delta) \right)^3 \quad (5)$$

where B_{xx} is the second virial coefficient for particles of the same species (assumed to be HS) and B_{xy} is the second virial coefficient of particles of different species, which can be HS or NAHS.

The general equation for the osmotic pressure for a dilute mixture is given by [9]:

$$\begin{aligned}\beta\Pi &= \rho + B_{11}\rho_1^2 + 2B_{12}\rho_1\rho_2 + 2B_{13}\rho_1\rho_3\ldots \\ &= \rho + \sum_i^n \sum_j^n B_{ij}\rho_i\rho_j + \ldots\end{aligned}\quad (6)$$

In this article we focus on binary mixtures in which one of the components consists of sub-components. By increasing the number of sub-components, the number of equations to solve for the phase diagram increases. Just as in article [9] we also compare the results to the number averaged virial coefficients of the different components. The number averaged virial coefficient was chosen because it allows for comparison to experiments, e.g. the virial coefficient obtained from osmometric measurements [16]. The number averaged second virial coefficient of a mixture can be written as:

$$\begin{aligned}B_{mix} &= B_{11}x_1^2 + 2B_{12}x_1x_2 + 2B_{13}x_1x_3\ldots \\ &= \sum_i^m \sum_j^m B_{ij}x_ix_j\end{aligned}\quad (7)$$

in which B_{ii} is the second virial coefficient of the i^{th} particle, B_{ij} is the second cross virial coefficient of the i^{th} particle and the j^{th} particle, and x_i is the fraction of the i^{th} particle, $\sum x_i = 1$.

Using this definition, we can map the binary mixture consisting of for example a monodisperse component 1 and a component 2 subdivided into two subcomponents (a and b) by a 2×2 matrix of virial coefficients. We will refer to this 2×2 matrix as the effective virial coefficient matrix.

$$\begin{aligned}B_{11_{eff}} &= B_{11} \\ B_{12_{eff}} &= x_a B_{12_a} + x_b B_{12_b} \\ B_{22_{eff}} &= x_a^2 B_{2a2a} + 2x_a x_b B_{2a2b} + x_b^2 B_{2b2b}\end{aligned}\quad (8)$$

The effective virial coefficient matrix for this mixture becomes then:

$$B_{eff} = \begin{bmatrix} B_{11_{eff}} & B_{12_{eff}} \\ B_{12_{eff}} & B_{22_{eff}} \end{bmatrix}\quad (9)$$

B. Stability of a mixture

The stability of a mixture is dependent on the second derivative of the free energy. If the second derivative of the mixture becomes zero, the mixture is at the boundary of becoming unstable. Unstable mixtures have a negative second derivative [17] [18].

The differential of the free energy of a mixture is given by [14]:

$$dA = -SdT - pdV + \sum_i^n \mu_i dN_i\quad (10)$$

in which μ_i , the chemical potential (the first partial derivative of the free energy with respect to number of particles (N_i)) for component i is given by:

$$\mu_i = \mu_i^0 + kT \ln(\rho_i) + 2kT \left(\sum_j^n B_{ij}\rho_j \right)\quad (11)$$

For a mixture with n distinguishable components, the second partial derivatives can be represented by a $n \times n$ matrix of the first partial derivatives of the chemical potential of each component.

This results in the following general stability matrix:

$$\begin{aligned}M_1 &= \begin{bmatrix} \frac{\partial \mu_1}{\partial N_1} & \cdots & \frac{\partial \mu_1}{\partial N_n} \\ \vdots & \ddots & \vdots \\ \frac{\partial \mu_n}{\partial N_1} & \cdots & \frac{\partial \mu_n}{\partial N_n} \end{bmatrix} \\ &= \begin{bmatrix} 2B_{11} + \frac{1}{\rho_1} & \cdots & 2B_{1n} \\ \vdots & \ddots & \vdots \\ 2B_{1n} & \cdots & 2B_{nn} + \frac{1}{\rho_n} \end{bmatrix}\end{aligned}\quad (12)$$

The mixture is stable when all eigenvalues are positive [19], when on the other hand one of the eigenvalues is not positive, the mixture becomes unstable. The limit of stability is reached when the matrix has one zero eigenvalue and is otherwise positive definite, and is referred to as the spinodal [20].

When there are only two components in the mixture ($n = 2$), the spinodal is defined by the condition $\det M_1 = 0$. When the number of components is larger ($n > 2$), $\det M_1 = 0$ can have more than one solution [19]. The spinodal can be found by checking whether $\det M_1$ changes sign for small changes in the concentrations of the components.

C. Critical points

In a binary mixture, the critical point is a stable point which lies on the stability limit (spinodal) [20] and where the phase boundary and spinodal coincide. In mixtures of more components these critical points become plait points. Critical points and plait points are in general concentrations at which two phases are in equilibrium and become indistinguishable [21].

There are two criteria that can be used to find critical points. The first one is $\det(M_1) = 0$, which is the equation for the spinodal. The other criterion is based on the fact that at the critical point, the third derivative of the

free energy should also be zero. For a multicomponent system, this criterion can be reformulated using Legendre transforms as $\det(M_2) = 0$ [18][22], where:

$$M_2 = \begin{bmatrix} \frac{\partial \mu_1}{\partial N_1} & \cdots & \frac{\partial \mu_n}{\partial N_n} \\ \vdots & \ddots & \vdots \\ \frac{\partial M_1}{\partial N_1} & \cdots & \frac{\partial M_1}{\partial N_n} \end{bmatrix} \quad (13)$$

Matrix M_2 is matrix M_1 with one of the rows replaced by the partial derivatives of the determinant of matrix M_1 . Note: it does not matter which row of the matrix is replaced.

D. Phase boundary

When a mixture becomes unstable and demixes into two or more phases, the chemical potential of each component and the osmotic pressure is the same in all phases [14].

$$\begin{cases} \beta\Pi^I = \beta\Pi^{II} = \cdots \\ \beta\mu_1^I = \beta\mu_1^{II} = \cdots \\ \vdots \\ \beta\mu_n^I = \beta\mu_n^{II} = \cdots \end{cases} \quad (14)$$

where the phases are denoted by I, II, \dots

For a mixture containing n distinguishable components, that demixes into two phases, this results in $n + 1$ equations and $2 \times n$ unknowns. If the mixture demixes into three phases, this results in $2 \times n + 2$ equations and $3 \times n$ unknowns. To solve the set of equations without having to fix the concentration of one component and the ratio between the other components for at least one of the phases, we need extra equations. For the extra set of equations, we build on the fact that no particles are lost and no new particles are created during phase separation, and the fact that we assume that the total volume does not change.

For a system that separates into three phases we then obtain:

$$\rho = \sum_i^n \rho_i = \frac{\sum_i^n N_i}{V} = \frac{\sum_i^n N_i^I + \sum_i^n N_i^{II} + \sum_i^n N_i^{III}}{V^I + V^{II} + V^{III}}$$

which can be rewritten as [9]:

$$\rho = \alpha^I \sum_i^n \rho_i^I + \alpha^{II} \sum_i^n \rho_i^{II} + (1 - \alpha^I - \alpha^{II}) \sum_i^n \rho_i^{III}$$

with

$$\alpha^I = \frac{V^I}{\sum_i^f V^i}$$

in which f denotes the number of phases. This results in the following set of equations:

$$\begin{cases} \beta\Pi^I = \beta\Pi^{II} = \cdots \\ \beta\mu_1^I = \beta\mu_1^{II} = \cdots \\ \vdots \\ \beta\mu_n^I = \beta\mu_n^{II} = \cdots \\ \rho_1 = \alpha^I \rho_1^I + \cdots + \left(1 - \sum_i^{f-1} \alpha^i\right) \rho_1^f \\ \vdots \\ \rho_n = \alpha^I \rho_n^I + \cdots + \left(1 - \sum_i^{f-1} \alpha^i\right) \rho_n^f \end{cases} \quad (15)$$

With this set of equations, we have $2 \times n + 1$ unknowns and $2 \times n + 1$ equations for mixtures that separate into two phases. For mixtures that demix into three phases, we have $3 \times n + 2$ unknowns and $3 \times n + 2$ equations. Therefore, this set of equations allows for calculating the concentration of each component in each of the phases for any given parent concentration, given that the mixture will demix at this concentration.

III. RESULTS AND DISCUSSION

In this work we calculated the phase diagram for a variety of binary non-additive mixtures of a small hard sphere A and a larger hard sphere B with a size ratio $q = \sigma_A/\sigma_B$. Component B is sub-divided into two sub-components and is characterized by a degree in polydispersity (PD), defined by:

$$PD = \frac{\sqrt{\sum (\sigma_{B_i} - \sigma_B)^2 \times N_{B_i}/N_B}}{\sigma_B} \times 100$$

We varied the non-additivity between particles of component A and B (Δ_{AB}), and between the sub-components of B ($\Delta_{B_a B_b}$). Next to that we varied the degree of polydispersity (PD) of component B and the distribution between the sub-components as well as the size ratio (q) between component A and B .

For all particles, the concentrations are expressed as a dimensionless parameter according to $\eta = \frac{\pi \rho \sigma^3}{6}$. We calculated the critical point, the phase separation boundary, and the spinodal of the various mixtures. Next to that, we also investigated the composition of the child phases, volume fraction of the phases (α), and the fractionation of the polydisperse component B for a specific parent mixture ($\eta = (0.010, 0.200)$), for mixtures with a size ratio $q = \sigma_A/\sigma_B = 1/10$ and $\Delta_{AB} = 0$, while varying the non-additive interaction between the sub-components of B ($\Delta_{B_a B_b}$).

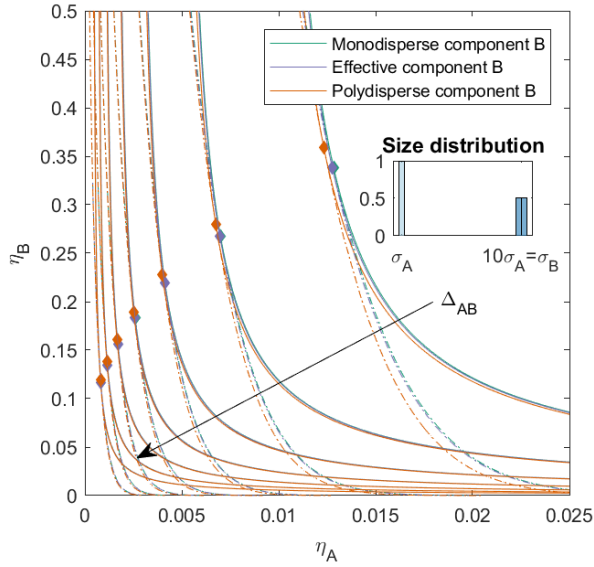


FIG. 1. Phase diagram for binary (component A and B) non-additive hard sphere mixture with size ratio $q = \sigma_A/\sigma_B = 1/10$, component A is monodisperse, component B is polydisperse ($PD = 4.00$), plotted as a function of the partial packing fractions, η_A and η_B . The interaction between components A and B is non-additive, the non-additivity parameter Δ_{AB} was varied from -0.1 to 0.5 with a step size of 0.1 (the arrow indicates increasing Δ_{AB}). The interaction between the sub-components B is additive. The spinodal (solid line) and binodal (dashed line) meet each other at the critical point (diamond).

A. Non-additive interaction between component A and B (Δ_{AB})

For the first set of mixtures (see figure 1), we calculated the phase diagram for binary mixtures with non-additive interaction between monodisperse component A and slightly polydisperse component B, with two sub-components and a $PD = 4.00$. These two sub-components are additive hard spheres in two sizes (both present in the same amount), with the number average size of the mixture equal to 10 times the size of component A. The mixture therefore consist of three components of different size. We varied the non-additivity between component A and B (Δ_{AB} , the same for both sub-components) from -0.1 to 0.5 with a step size of 0.1. When $\Delta_{AB} = 0$, the interaction between all components equals additive hard sphere interaction. We calculated the phase diagram using both the simplified 2×2 effective virial coefficient matrix described in the theory (we refer to this as the effective mixture B) and the full 3×3 virial coefficient matrix (to which we refer as the polydisperse mixture B). These mixtures are also compared to mixtures in which component B is monodisperse with a size equal to the average particle size of component B (we refer to this as the monodisperse mixture B).

With increasing Δ_{AB} , the phase boundary, spinodal and

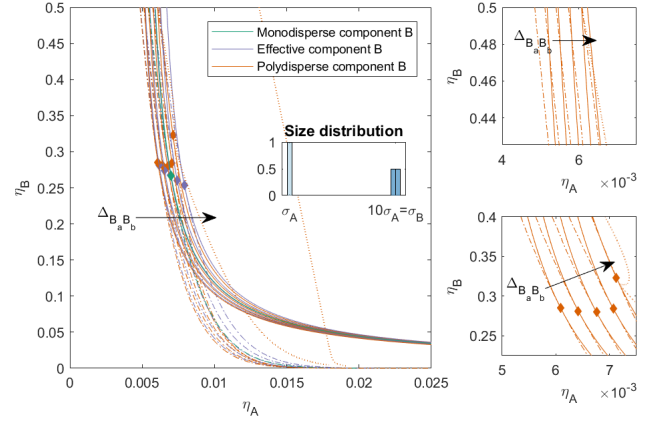


FIG. 2. Phase diagram for binary (component A and B) non-additive hard sphere mixture with size ratio $q = \sigma_A/\sigma_B = 1/10$, component A is monodisperse, component B is polydisperse ($PD = 4.00$), plotted as a function of the partial packing fractions, η_A and η_B . The interaction between components A and B is additive, the interaction between the sub-components B is non-additive, the non-additivity parameter $\Delta_{B_a B_b}$ was varied from -0.1 to 0.1 with a step size of 0.05 (the arrow indicates increasing $\Delta_{B_a B_b}$). The spinodal (solid line) and binodal (dashed line) meet each other at the plait point (diamond), the three phase boundary is indicated with a dotted line and meets the spinodal at the plait point (diamond).

critical point shifts towards lower concentrations, for the monodisperse mixture, effective mixture, and polydisperse mixture. This is in line with research on non-additive binary mixtures [23]. The difference between the phase boundary, spinodal and critical point of the monodisperse mixture and the effective mixture is negligible, for all Δ_{AB} . We see however that the introduction of the polydispersity causes the critical point to shift to a higher volume fraction of component B and that especially at lower volume fraction of component B the phase separation boundary shifts towards slightly lower packing fractions. This effect is more pronounced when Δ_{AB} is small.

When the PD of component B is increased, or the distribution of the sub-components of B is varied, we see the same pattern as in figure 1 (see supplementary materials). However, we see that, just like discussed in [9], the critical point shifts towards higher concentrations of B for the polydisperse mixtures depending on the size and concentration of the largest sub-component of B and the difference between the effective and the monodisperse mixtures increases with the size of the largest sub-component of B.

B. Non-additive interaction within polydisperse component B ($\Delta_{B_a B_b}$)

In the next set of mixtures, we kept the interaction between the components A and B as hard-sphere addi-

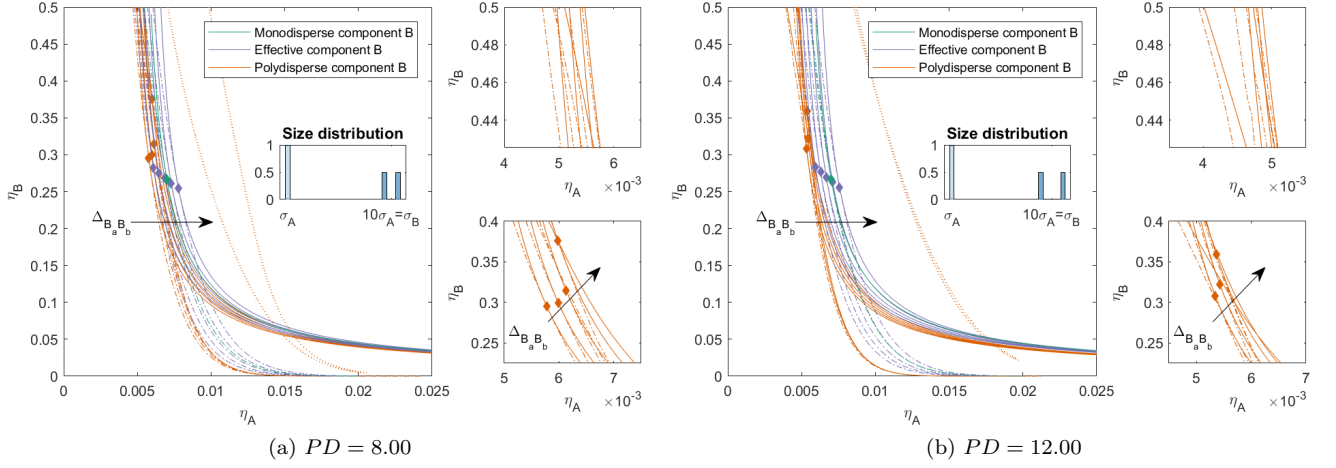


FIG. 3. Phase diagram for binary (component A and B) non-additive hard sphere mixture with size ratio $q = \sigma_A/\sigma_B = 1/10$, component A is monodisperse, component B is polydisperse ($PD = 8.00$ or $PD = 12.00$), plotted as a function of the partial packing fractions, η_A and η_B . The interaction between components A and B is additive, the interaction between the sub-components B is non-additive, the non-additivity parameter $\Delta_{B_a B_b}$ was varied from -0.1 to 0.1 with a step size of 0.05 (the arrow indicates increasing $\Delta_{B_a B_b}$). The spinodal (solid line) and binodal (dashed line) meet each other at the plait point (diamond), the three phase boundary is indicated with a dotted line.

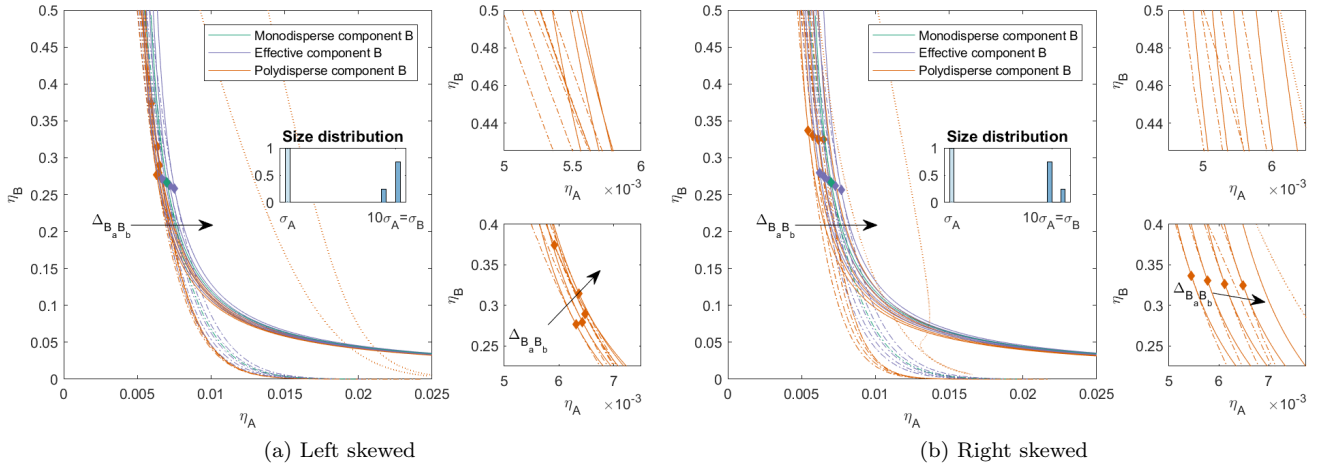


FIG. 4. Phase diagram for binary (component A and B) non-additive hard sphere mixture with size ratio $q = \sigma_A/\sigma_B = 1/10$, component A is monodisperse, component B is polydisperse ($PD = 6.93$), plotted as a function of the partial packing fractions, η_A and η_B . The interaction between components A and B is additive, the interaction between the sub-components B is non-additive, the non-additivity parameter $\Delta_{B_a B_b}$ was varied from -0.1 to 0.1 with a step size of 0.05 (the arrow indicates increasing $\Delta_{B_a B_b}$). The spinodal (solid line) and binodal (dashed line) meet each other at the plait point (diamond), the three phase boundary is indicated with a dotted line.

tive, but we introduced some non-additivity in the interaction between the sub-components of B . we varied $\Delta_{B_a B_b}$ from -0.10 to 0.10 with a step size of 0.05 . When $\Delta_{B_a B_b}$ is small, the sub-components are more compatible with each other, when on the other hand $\Delta_{B_a B_b}$ increases and becomes positive, the compatibility between the sub-components decreases. When $\Delta_{B_a B_b} > 0$ it becomes possible for components of similar size to phase separate [23].

In figure 2 we plotted the phase diagram for the binary

mixtures with $PD = 4.00$, $\Delta_{AB} = 0$ and we varied $\Delta_{B_a B_b}$. When $\Delta_{B_a B_b} > 0$, the compatibility between the sub-components decreases and phase separation into three phases becomes possible (depicted as the dotted line in the figure). Mixtures with a smaller $\Delta_{B_a B_b}$ demix into two phases at lower concentrations compared to the completely hard sphere mixture. Mixtures with a larger $\Delta_{B_a B_b}$ demix into two phases at higher packing fractions compared to the completely hard sphere mixture, and also have a three phase boundary. The three-phase

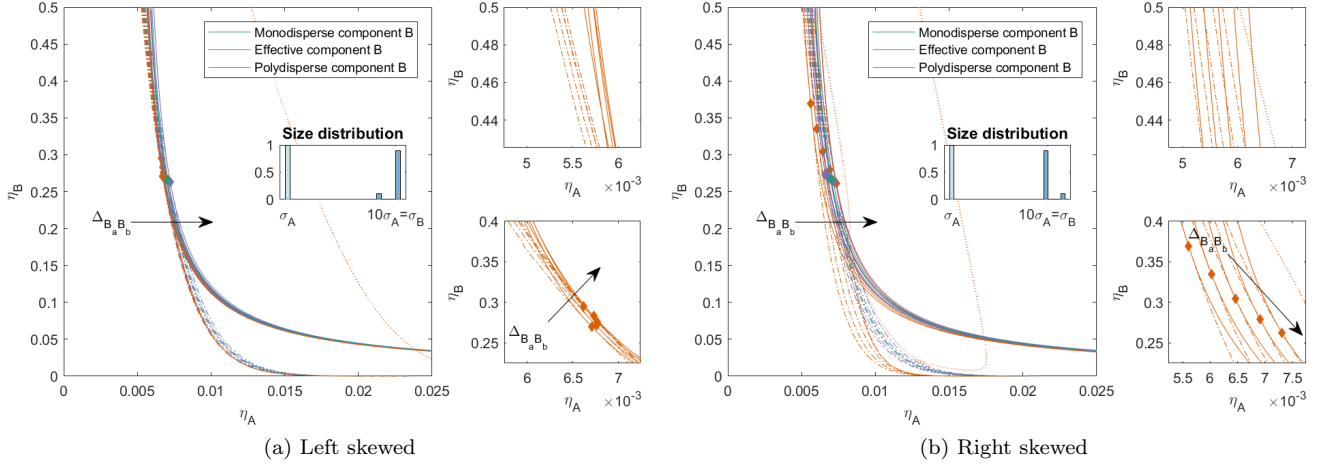


FIG. 5. Phase diagram for binary (component A and B) non-additive hard sphere mixture with size ratio $q = \sigma_A/\sigma_B = 1/10$, component A is monodisperse, component B is polydisperse ($PD = 4.80$), plotted as a function of the partial packing fractions, η_A and η_B . The interaction between components A and B is additive, the interaction between the sub-components B is non-additive, the non-additivity parameter $\Delta_{B_a B_b}$ was varied from -0.1 to 0.1 with a step size of 0.05 (the arrow indicates increasing $\Delta_{B_a B_b}$). The spinodal (solid line) and binodal (dashed line) meet each other at the plait point (diamond), the three phase boundary is indicated with a dotted line.

boundary is at lower concentrations for larger $\Delta_{B_a B_b}$ and comes close to the two-phase boundary for the mixture with $\Delta_{B_a B_b} = 0.10$. The critical point of the polydisperse mixtures changes depending on the non-additivity of the sub-components: The critical point is at its lowest concentrations of A for negative $\Delta_{B_a B_b}$, its lowest concentration of B is when the interaction between the sub-components of B becomes more like HS, and the concentration of the critical point for B increases with $\Delta_{B_a B_b}$. In figure 3 we increased the PD for component B to 8.00 and 12.00 respectively, we kept $\Delta_{AB} = 0$ and we varied $\Delta_{B_a B_b}$ as before. With increased PD , the two-phase boundary of the polydisperse mixture shifts towards lower packing fractions for all mixtures. The effect of $\Delta_{B_a B_b}$ on the position of the two-phase boundary becomes smaller at lower concentration of B , however at higher concentrations of B we see that the two-phase boundary for positive $\Delta_{B_a B_b}$ bends towards the y -axis and this effect is more pronounced for higher PD . The polydispersity of B also has an effect on the position of the three-phase boundary. With increased PD , the position of the three-phase boundary becomes less dependent on $\Delta_{B_a B_b}$ and the difference in the position of the two-phase boundary and the three-phase boundary increases for the mixtures with $\Delta_{B_a B_b} = 0.10$. For the mixtures with $PD = 12.00$, the difference between the three-phase boundary for the mixtures that phase separate into three phases becomes negligible. We see similar trends in the critical points for the more polydisperse mixture as in figure 2, however, with increased polydispersity and especially increased incompatibility between the sub-components ($\Delta_{B_a B_b} > 0$), the critical point shifts towards higher concentrations of B . For the mixtures with larger $\Delta_{B_a B_b}$, the critical point can shift

to $\eta_{B_{crit}} > 0.5$.

In figure 4 and 5 we varied the ratio between the sub-components of B . The ratio between the sub-components of B is $25/75$ with a $PD = 6.93$ in figure 4 (both left and right skewed) and $10/90$ with a $PD = 4.80$ in figure 5 (both left and right skewed). These mixtures can be seen as a model for mixtures that contain some impurities, from a similar material but at different size when $\Delta_{B_a B_b} = 0$ or a material that is less compatible with the main component (when $\Delta_{B_a B_b} > 0$) or more compatible with the main component (when $\Delta_{B_a B_b} < 0$). The PD is the same for both the left skewed and the right skewed mixtures. For both types of mixtures, we see that the two-phase boundaries are closer to each other for the left-skewed mixtures (large amount of the largest sub-component) compared to the right-skewed mixtures. Next to that, these left-skewed mixtures also show a larger bend in the two-phase boundary towards the y -axis for $\Delta_{B_a B_b} > 0$. The mixture in figure 5a with $\Delta_{B_a B_b} = 0.05$ does not have a three phase boundary, even though mixtures with these sizes can phase separate into three phases: the distribution of the sub-components makes these concentrations unattainable in the range of concentrations we focus on.

For the right-skewed mixtures, we see that the three-phase boundary for mixtures with $\Delta_{B_a B_b} = 0.10$ comes very close to the two-phase boundary and for mixtures with $\Delta_{B_a B_b} = 0.05$ the three phase boundary shows a bend back towards lower concentrations of A at low concentrations of B . This is due to the shape of the three-phase surface and can also be seen on a small level in the mixture $\Delta_{B_a B_b} = 0.10$ in figure 2.

Also Bellier-Castella and coauthors [24] found the possibility of three phase separation for polydisperse com-

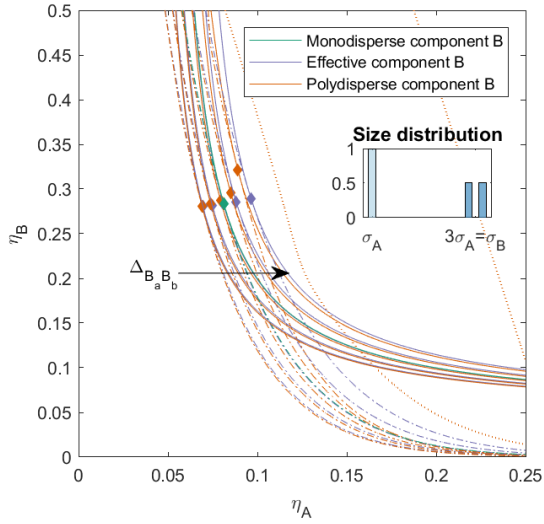


FIG. 6. Phase diagram for binary (component A and B) non-additive hard sphere mixture with size ratio $q = \sigma_A/\sigma_B = 1/3$, component A is monodisperse, component B is polydisperse ($PD = 4.00$), plotted as a function of the partial packing fractions, η_A and η_B . The interaction between components A and B is non-additive with a non-additivity parameter $\Delta_{AB} = 0.075$, the interaction between the sub-components B is non-additive, the non-additivity parameter $\Delta_{B_a B_b}$ was varied from -0.1 to 0.1 with a step size of 0.05 (the arrow indicates increasing $\Delta_{B_a B_b}$). The spinodal (solid line) and binodal (dashed line) meet each other at the plait point (diamond), the three phase boundary is indicated with a dotted line.

ponents. According to them, the transition between the two phase and three phase region proceeds via a second critical point. This second critical point is polydispersity induced.

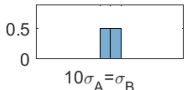
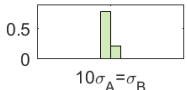
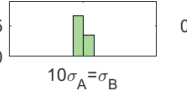
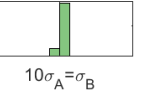
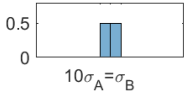
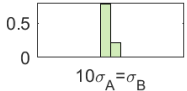
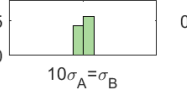
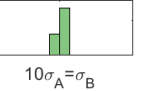
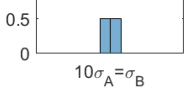
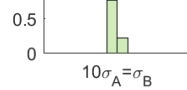

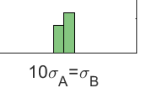
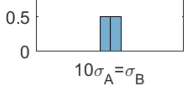


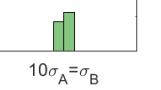
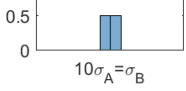
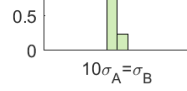

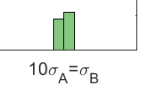
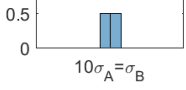


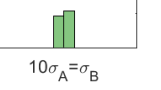
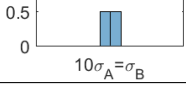
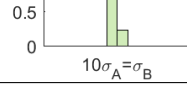

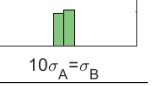
C. Mixtures with non-additivity between sub-components of B ($\Delta_{B_a B_b}$), and between A and B (Δ_{AB})

In figure 6 we plot the phase diagram for mixtures with varying $\Delta_{B_a B_b}$, with a size ratio between component A and B of $q = 1/3$, and a non-additive interaction between A and B $\Delta_{AB} = 0.075$. This is in fact a combination of the case in section III A and III B at lower size ratio between A and B . The polydispersity of B is 4.00 (for mixtures with more variety in PD and Δ_{AB} we refer to supplementary material). The phase diagram of these mixtures shows a lot of similarities with the phase diagram of the mixtures in figure 2 though at different η_A due to the different size ratio. Since the mixtures in figure 2 have the same PD , we conclude that the three-phase boundary position and shape is largely dependent on the interaction between the sub-components of B . The interaction between the sub-components is determined by both the PD and the non-additivity parameter $\Delta_{B_a B_b}$.

TABLE I. Critical points for the different binary mixtures depending on the non-additivity of component B , see also figure 2 and phase separated concentrations and volume fraction α of the different mixtures for specific parent concentration ($\eta_{Aparent} = 0.010$, $\eta_{Bparent} = 0.200$), depending on the non-additivity of component B see II for distribution of component B in each phase.

$\Delta_{B_a B_b}$	η_{crit}	Top phase	Middle phase	Bottom phase
0.100	(0.007, 0.323)	η (0.011, 0.074) PD: 3.35, Size: 0.97, α : 0.817	η (0.006, 0.596) PD: 3.84, Size: 0.99, α : 0.097	η (0.004, 0.953) PD: 2.62, Size: 1.03, α : 0.087
0.0875	(0.007, 0.303)	η (0.011, 0.064) PD: 3.39, Size: 0.98, α : 0.804	η (0.005, 0.733) PD: 3.94, Size: 1.01, α : 0.138	η (0.004, 0.813) PD: 3.65, Size: 1.02, α : 0.058
0.075	(0.007, 0.294)	η (0.011, 0.057) PD: 3.42, Size: 0.98, α : 0.799		η (0.005, 0.767) PD: 3.91, Size: 1.01, α : 0.201
0.05	(0.007, 0.285)	η (0.011, 0.047) PD: 3.44, Size: 0.98, α : 0.797		η (0.004, 0.800) PD: 3.94, Size: 1.01, α : 0.203
0	(0.007, 0.280)	η (0.011, 0.034) PD: 3.45, Size: 0.98, α : 0.804		η (0.004, 0.881) PD: 3.97, Size: 1.00, α : 0.196
-0.05	(0.006, 0.281)	η (0.011, 0.026) PD: 3.45, Size: 0.98, α : 0.815		η (0.004, 0.966) PD: 3.98, Size: 1.00, α : 0.185
-0.1	(0.006, 0.285)	η (0.011, 0.020) PD: 3.45, Size: 0.98, α : 0.825		η (0.003, 1.051) PD: 3.99, Size: 1.00, α : 0.175

TABLE II. Phase separation of different mixtures and fractionation of component B for specific parent distribution ($\eta_{A_{parent}} = 0.010, \eta_{B_{parent}} = 0.200$), depending on the non-additivity of component B , see also figure 2

$\Delta_{B_a B_b}$	Parent distribution	Top phase	Middle phase	Bottom phase
0.1				
0.0875				
0.075				
0.05				
0				
-0.05				
-0.1				

D. Fractionation

When a parent mixture demixes into two or more phases, each component (and also their sub-components) in the mixture will find its preferential phase in order to minimize the Helmholtz free energy of the system. This leads each phase to be enriched in one of the components, whilst being depleted by the other component(s). The other component(s) are then present only at low volume fractions. We investigated the phase separation for the mixtures in section IIIB for a specific parent mixture ($\eta_{A_{parent}} = 0.010, \eta_{B_{parent}} = 0.200$) in terms of the volume fraction of both components in each phase, the degree of polydispersity of component B , average size of component B in the child phases compared to the average size of component B in the parent phase and the volume fraction of the phases (α) see table I for the mixtures from figure 2 (mixtures with $PD = 4.00$), for other mixtures we refer to the supplementary materials. The composition histograms for each phase are given in table II for the same mixture, for other mixtures we refer to the supplementary materials. Since at this parent concentration the mixture with non-additivity parameter $\Delta_{B_a B_b} = 0.10$ separates into three phases, we have also calculated the

child phases for mixtures with between $\Delta_{B_a B_b} = 0.10$ and $\Delta_{B_a B_b} = 0.05$ to investigate the behavior of the sub-components B depending on the non-additivity.

For all mixtures, the top phase, which is also the largest phase in volume, is enriched in component A . The volume fraction of the top phase is dependent on the non-additive interaction between the sub-components of B . It increases with both more compatibility between the sub-components as well as less compatibility, with a minimum volume fraction at $\Delta_{B_a B_b} = 0.05$. We find this dependence in volume fraction on the non-additivity parameter $\Delta_{B_a B_b}$ also for the other mixtures, however the minimum volume fraction is at different $\Delta_{B_a B_b}$ depending on the sizes of and the ratio of the sub-components a and b of B . For the mixtures ($\Delta_{B_a B_b} > 0.075$) that phase separate into three phases at this parent mixture concentration, we conclude that it is mostly the bottom phase that demixes into an additional phase (the middle phase). The bottom phase is enriched in the largest sub-component of B , while the top phase (and middle phase to a lesser extent) is enriched in the smaller sub-component of B . We see this behavior also for the other mixtures with different composition of B .

The fractionation of the sub-components of B is dependent on the non-additivity parameter $\Delta_{B_a B_b}$. When $\Delta_{B_a B_b} < 0$ the sub-components a and b are more compatible with each other and this leads to less fractionation, as can be seen in table II, while on the other hand $\Delta_{B_a B_b} > 0$ the sub-components are less compatible with each other and more fractionation occurs, even leading to additional phase separation at higher $\Delta_{B_a B_b}$. This is something we see also for the other mixtures (see supplementary material).

IV. CONCLUSION

We find that when the compatibility between component A and B is decreased, the phase diagram (the critical point, phase boundary and spinodal) shifts towards lower volume fractions. This is in line with literature on the phase behavior of NAHS binary monodisperse mixtures. The interaction between A and B is driven by the size ratio (q) between A and B and the non-additivity parameter Δ_{AB} .

When the compatibility between the sub-components of the polydisperse component B is altered, the phase diagram changes more drastically. When the compatibility between the sub-components is decreased, the mixture can demix into three phases each enriched in one of the (sub)components of the parent mixture. The shape and position of the three phase boundary is mainly depen-

dent on the interactions between the sub-components of B . This means that it is dependent on the non-additivity parameter ($\Delta_{B_a B_b}$) as well as the size ratios and distribution of the sub-components (the degree of polydispersity PD). Next to that, depending on the size ratios and distribution of the sub-components we see also that the binodal and spinodal bend towards the y-axis for higher volume fractions of B when $\Delta_{B_a B_b}$ increases. For the mixtures with a more pronounced bend in the phase boundary and spinodal, we find that the critical point shifts to volume fractions $\eta_{B_{crit}} > 0.5$. This behavior is driven to a large extent by the non-additivity parameter ($\Delta_{B_a B_b}$) as well as the size ratios and distribution of the sub-components (the degree of polydispersity PD) and to a lesser extent by the interaction between A and B . When the compatibility between the sub-components is increased, the mixture demixes at slightly lower packing fractions compared to the HS mixture. The fractionation of the polydisperse sub-components of B is also dependent on the non-additivity parameter $\Delta_{B_a B_b}$. Less fractionation occurs when $\Delta_{B_a B_b} < 0$, more fractionation occurs when $\Delta_{B_a B_b} > 0$. At higher $\Delta_{B_a B_b}$ this can even lead to additional phase separation, creating a third phase.

The virial coefficient approach for polydisperse mixtures allows for the prediction of the phase behavior of polydisperse or impure binary mixtures. Not only does it allow for plotting the phase diagram, it also allows for the calculation of the composition and fractionation of each component in each phase.

-
- [1] W. F.C. Sager. Systematic study on the influence of impurities on the phase behavior of sodium bis(2-ethylhexyl) sulfosuccinate microemulsions. *Langmuir*, 14(22):6385–6395, 1998.
 - [2] Marijke W. Edelman, Erik van der Linden, Els de Hoog, and R. Hans Tromp. Compatibility of Gelatin and Dextran in Aqueous Solution. *Biomacromolecules*, 2(4):1148–1154, dec 2001.
 - [3] V. Kontogiorgos, S. M. Tosh, and P. J. Wood. Phase behaviour of high molecular weight oat β -glucan/whey protein isolate binary mixtures. *Food Hydrocolloids*, 23(3):949–956, 2009.
 - [4] Thierry Biben and Jean-Pierre Hansen. Osmotic depletion, non-additivity and phase separation. *Physica A: Statistical Mechanics and its Applications*, 235(1-2):142–148, jan 1997.
 - [5] T. Biben and Hansen Jean-Pierre. Spinodal instability of suspensions of large spheres in a fluid of small spheres. *Journal of Physics: Condensed Matter*, 3(42):F65–F72, oct 1991.
 - [6] Marjolein Dijkstra, René van Roij, and Robert Evans. Phase diagram of highly asymmetric binary hard-sphere mixtures. *Physical Review E - Statistical Physics, Plasmas, Fluids, and Related Interdisciplinary Topics*, 59(5):5744–5771, 1999.
 - [7] R. Roth, R. Evans, and A. A. Louis. Theory of asymmetric nonadditive binary hard-sphere mixtures. *Physical Review E - Statistical Physics, Plasmas, Fluids, and Related Interdisciplinary Topics*, 64(5):13, 2001.
 - [8] Marjolein Dijkstra. Phase behavior of nonadditive hard-sphere mixtures. *Physical Review E - Statistical Physics, Plasmas, Fluids, and Related Interdisciplinary Topics*, 58(6):7523–7528, 1998.
 - [9] Luka Sturtewagen and Erik van der Linden. Effect of polydispersity on the phase behavior of additive hard spheres in solution, part I. *Manuscript submitted*, 2019.
 - [10] Martin Piech and John Y. Walz. Effect of Polydispersity and Charge Heterogeneity on the Depletion Interaction in Colloidal Systems. *Journal of Colloid and Interface Science*, 225(1):134–146, may 2000.
 - [11] Per Sillren and Jean Pierre Hansen. On the critical non-additivity driving segregation of asymmetric binary hard sphere fluids. *Molecular Physics*, 108(1):97–104, 2010.
 - [12] Patrice Paricaud. Phase equilibria in polydisperse nonadditive hard-sphere systems. *Physical Review E*, 78(2):021202, aug 2008.
 - [13] Richard P. Sear and Daan Frenkel. Phase behavior of colloid plus polydisperse polymer mixtures. *Physical Review E - Statistical Physics, Plasmas, Fluids, and Related Interdisciplinary Topics*, 55(2):1677–1681, feb 1997.
 - [14] Terrel L. Hill. *An Introduction to Statistical Thermodynamics*. Dover Publications, New York, 1986.
 - [15] Henk N.W. Lekkerkerker and Remco Tuinier. *Colloids and the Depletion Interaction*, volume 833. 2011.

- [16] Carsten Ersch, Erik van der Linden, Anneke Martin, and Paul Venema. Interactions in protein mixtures. Part II: A virial approach to predict phase behavior. *Food Hydrocolloids*, 52:991–1002, 2016.
- [17] Robert A. Heidemann. The criteria for thermodynamic stability. *AIChE Journal*, 21(4):824–826, jul 1975.
- [18] Bruce L. Beegle, Michael Modell, and Robert C. Reid. Thermodynamic stability criterion for pure substances and mixtures. *AIChE Journal*, 20(6):1200–1206, nov 1974.
- [19] M. A. Solokhin, A. V. Solokhin, and V. S. Timofeev. Phase-equilibrium stability criterion in terms of the eigenvalues of the Hessian matrix of the Gibbs potential. *Theoretical Foundations of Chemical Engineering*, 36(5):444–446, 2002.
- [20] Robert A. Heidemann and Ahmed M. Khalil. The calculation of critical points. *AIChE Journal*, 26(5):769–779, sep 1980.
- [21] Robert A. Heidemann. The Classical Theory of Critical Points. In *Supercritical Fluids*, pages 39–64. Springer Netherlands, Dordrecht, 1994.
- [22] Robert C. Reid and Bruce L. Beegle. Critical point criteria in legendre transform notation. *AIChE Journal*, 23(5):726–732, sep 1977.
- [23] Paul Hopkins and Matthias Schmidt. Binary non-additive hard sphere mixtures: Fluid demixing, asymptotic decay of correlations and free fluid interfaces. *Journal of Physics Condensed Matter*, 22(32), 2010.
- [24] L. Bellier-Castella, H. Xu, and M. Baus. Phase diagrams of polydisperse van der Waals fluids. *Journal of Chemical Physics*, 113(18):8337–8347, 2000.